

# Investigating Factors Affecting the Resonant Frequency of Cantilever Beams

**Research Question:** To what extent does changing the length of a circular cantilever beam affect its resonant frequency, and how well can the theoretical model predict this relationship?

International Baccalaureate Physics Extended Essay

Word Count:3985

# Table Of Contents

Table Of Contents	I
1 Introduction	1
2 Background Information	2
2.1 Euler–Bernoulli Beam Theory . . . . .	2
2.2 Finite Element Method . . . . .	3
2.3 Fourier Transform . . . . .	4
3 Methodology	5
3.1 Theory . . . . .	5
3.2 Finite Element Analysis . . . . .	6
3.3 Experiment . . . . .	10
4 Results And Analysis	15
4.1 Uncertainty Analysis . . . . .	15
5 Discussion	16
6 Conclusion	17
References	19

# 1 Introduction

Cantilever beams, seemingly simple elements used in construction where one end of a beam is solidly attached and the other loose, has played a major role in engineering, historically, these structures were used for purely mechanical structures, such as buildings, cranes, balconies and bridges (Hool and Johnson 1929).

While the use of such simple elements is still common in traditional construction, their range of use expands far beyond macroscopic architecture, Nowadays cutting edge technology such as MEMS(micro-electromechanical) systems which integrate mechanical systems with electronics in a microscopic level, use such structures as well, such as microscopic cantilever beams are that are used as inertial sensors in gyroscopes to sense the tiny acceleration forces in various circumstances (Bao 2005).

I was fascinated to learn that such simple structures lie at the core of technologies we take for granted today. This pushed me to further investigate their functionality and their dynamic properties. My research question is “To what extent does changing the length of a circular cantilever beam affect its resonant frequency, and how well can the theoretical model predict this relationship?” and I aim to determine how the length of the beam and the initial energy loaded into the beam will affect the frequency that the beam naturally vibrates at when excited using pure mathematics and experimentally. In addition to proving it mathematically and experimentally, I also intend to conduct a virtual experiment, using Finite Element Analysis. As shown in (1), I am expecting to see the frequency is inversely proportional to the square of its length, and to see no meaningful

relationship between the frequency and the initial energy load.

$$\begin{aligned} f_n &\propto \frac{1}{l^2} \\ f_n &\not\propto E_{initial} \end{aligned} \tag{1}$$

Where  $f_n$  is the natural frequency,  $l$  is the length of the beam and  $E_{initial}$  is the amount of energy used to excite the beam.

I intend to derive the hypothesis (1) in Section 3.1 and show it to be true in Section 3.2 and Section 3.3 Using computational dynamics and an experiment respectively, and discuss the results, potential errors in methodology and what could be improved in Section 4.

## 2 Background Information

### 2.1 Euler–Bernoulli Beam Theory

To analyze bending of thin beams with axial loads, the Euler–Bernoulli Beam Theory, also known as classic beam theory is commonly used. This theory, forming the basis of a lot of engineering formulae. This theory assumes the beam deformation comes mainly from the bending moment, with a negligible amount of shear deformation. The formula is generally expressed as a fourth order linear differential equation, allowing deflection to be calculated from applied load, flexural rigidity and the loads positioning on the beam. Solving this equation gives the deflection curve, enabling the calculation of stresses, shear forces and bending moments (Gross et al. 2014). There lie assumptions behind this theory, including isotropic(same in all directions) material behavior and uniform density which can be assumed true for high carbon steel such as the ones that are that are used in this experiment.(Gross et al. 2014) As this theorem does not take shear deformation into account, the beam needs to be thin relative to its length so the shear forces become negligible, as such, the size of the beams have been specifically picked to avoid shear forces. As this theorem

is only able to calculate static loads, we will further expand it on Section 3.1 to derive the dynamic beam equation.

## **2.2 Finite Element Method**

In engineering, it is common to be faced with partial differential equations, these equations are usually complex and are computationally intense to calculate, for example, calculating heat transfer, fluid flow, or in the case of this paper, non-rigid bodies. The Finite Element Method(FEM) is a way method to estimate the result of the partial differential equation, by dividing the continuous space of the problem into smaller, discrete parts called finite elements.

The collection of the finite elements is known as the mesh. By dividing the space, analysis within each element becomes simpler, and later combined to get an estimation, this allows the computation of the differential equations to be computationally simpler. As this is a method of estimation, the results are not always accurate, to get the estimate closer to reality, the mesh resolution is increased at the cost of compute time (Zienkiewicz and Taylor 2000).

The use of this method of engineering analysis is commonly known as Finite Element Analysis(FEA) and will be used as a virtual experiment in Section 3.2 to simulate the cantilever beams natural frequency. As this method allows to simulate deformation of bodies, this tool is generally built into Computer Aided Design (CAD) suites and Onshape, a cloud based CAD suite will be used in this paper.

## 2.3 Fourier Transform

The Fourier Transform (FT) is a fundamental mathematical technique used to break down time domain functions into their individual frequencies, essentially allowing to break a function down to its individual frequency components, indicating each frequencies amplitude and phase present in the original function.

The mathematical principle behind the Fourier Transform is based on representing signals as a sum of cyclic functions, specifically sine and cosine. Any periodic signal is able to be represented as a sum of the sine and cosine functions, each with a unique amplitude and phase. This allows to break down a signal into its individual frequencies. In practice, continuous data sets cannot be attained, so the Discrete Fourier Transform is used. The Discrete Fourier Transform is the discrete counterpart of the traditional Fourier Transform, allowing it to work on finite data sets such as those attained in experimentation or communications. The Discrete Fourier Transform algorithm transforms a finite, equally spaced set of data in the time domain into a sequence of Discrete Fourier Transform coefficients, each representing the amplitude and frequency that when combined, makes up the signal. One of the major drawbacks of the Discrete Fourier Transform algorithm is its computational intensity, for that, the Fast Fourier Transform is used, the Fast Fourier Transform, instead of being a differential transform, is a computationally optimized recursive algorithm. Allowing for the Discrete Fourier Transform to of a signal to be calculated with much less compute power, this is especially useful for large data sets since the computational complexity of calculating the Discrete Fourier Transform is exponential with the datasets length (Rao, Kim, and Hwang 2011).

For the specific purpose of analyzing a sound recording and breaking it down to its individual frequencies, the Fast Fourier Transform provides a direct and efficient way. By

transforming the data formatted as pressure-time to the frequency domain, attaining frequency-amplitude data that allows us to see the dominant frequencies making up the signal, and this case, the dominant frequency will be the resonant frequency of the cantilever beam.

## 3 Methodology

### 3.1 Theory

In Section 2.1, the static beam theory was introduced. Now, to determine the relationship for the resonant frequency of a cantilever beam, will be derived aiming to show its inverse square proportionality to length and independence from initial energy, as hypothesized in (1).

Starting with the Static Beam Equation (2):

$$\frac{d^2}{dx^2}(EI \frac{d^2w}{dx^2}) = q(x) \quad (2)$$

Where  $x$  is the point along the beam,  $E$  is the Young's modulus,  $I$  is the second moment of area and  $q(x)$  is the force applied to the model at point  $x$

To consider dynamics, the static load  $q(x)$  is replaced with the inertial force per unit length,  $-\rho A \frac{\partial^2 w(x,t)}{\partial t^2}$ , leading to the Dynamic Beam Equation for unconstrained vibration:

$$EI \frac{\partial^4 w(x,t)}{\partial x^4} + \rho A \frac{\partial^2 w(x,t)}{\partial t^2} = 0 \quad (3)$$

Assuming constant flexural rigidity  $EI$ . For natural frequencies, harmonic motion is assumed as:  $w(x,t) = W(x) \cos(\omega t)$ , where  $\omega$  is the angular velocity. Substituting this into (3) and simplifying gives the spatial ordinary differential equation:

$$EI \frac{d^4 W(x)}{dx^4} - \rho A \omega^2 W(x) = 0 \quad (4)$$

Letting  $\beta^4 = \frac{\rho A \omega^2}{EI}$ :

$$\frac{d^4 W(x)}{dx^4} - \beta^4 W(x) = 0 \quad (5)$$

Where  $\beta$  is the spatial frequency parameter.

For a cantilever beam, boundary conditions are: at the fixed end ( $x = 0$ ),  $W(0) = 0$  and  $W'(0) = 0$ ; at the free end ( $x = l$ ),  $W''(l) = 0$  and  $W'''(l) = 0$ . Solving this eigenvalue problem gives solutions for specific  $\beta$  values, determining natural frequencies  $\omega_n$ . For the fundamental mode,  $\beta_1 l \approx 1.875$ .

Since  $\beta^4 = \frac{\rho A \omega^2}{EI} = \frac{\rho A (2\pi f)^2}{EI}$ , we have  $\beta \propto \sqrt{f}$  with frequency  $f$ . Combined with  $\beta_1 l \approx$  constant, this leads to  $\sqrt{f_1} l \approx$  constant, and squaring both sides gives:

$$f_1 \propto \frac{1}{l^2} \quad (6)$$

This confirms the relationship between frequency  $f$  and length  $l$ . The proportionality constant depends on material ( $E, \rho$ ) and geometry ( $I, A$ ), and is kept constant in throughout the experiments.

Regarding the second part of the hypothesis, frequency is a property of the system, determined by material and dimensions. Initial energy affects vibration amplitude, not frequency. The frequency is set by length. Thus, resonant frequency is theoretically independent of initial energy, supporting the hypothesis.  $f_n \not\propto E_{initial}$  (Gross et al. 2014).

### 3.2 Finite Element Analysis

As explained in Section 2.2, FEA is a method to compute partial differential equations, and as shown in Section 3.1 the resonant frequencies of the beam can be calculated with an partial differential equation. Thankfully, there exists tools to calculate the Finite Element Model built-in on many CAD suites to make the calculations, in this case, PTC's Onshape



is to be used.

To start, we need to define the variables and constants.

$$\begin{aligned}
\varnothing &= 22mm \\
l_1 &= 200mm \\
l_2 &= 150mm \\
l_3 &= 100mm \\
E_1 &= 5 \text{ J} \\
E_2 &= 7.5 \text{ J} \\
E_3 &= 10 \text{ J}
\end{aligned} \tag{7}$$

As shown in (7), The diameter  $\varnothing$ , length  $l$  and initial energy  $E$  have been picked according to commonly available materials and for ease of assess, the lengths picked should also be able to give a wide variety of frequencies. Additionally, the material properties of hardened carbon steel are required to run the simulation, shown in (8), these values were taken from Onshape.

$$\begin{aligned}
\rho &= 7.850 \times 10^{-6} \frac{kg}{mm^3} \\
\nu &= 0.292 \\
E &= 200000000000 \text{ Pa}
\end{aligned} \tag{8}$$

Where  $\rho$  is the Density,  $\nu$  is Poisson's ratio and  $E$  is Young's Modulus

Variable	Length $l$	Energy $E$	Deformation $\epsilon$	Frequency $f$
Type	Independent	Independent	Dependent	Dependent
	Discrete	Discrete	Continuous	Continuous
Unit	mm	J	mm	Hz, $s^{-1}$

Table 1: Table of Variables for the Simulation

The table of variables, is shown in Table 1. The length  $l$  and energy  $E$  will be changed according to (7) and a separate simulation will be ran for each.

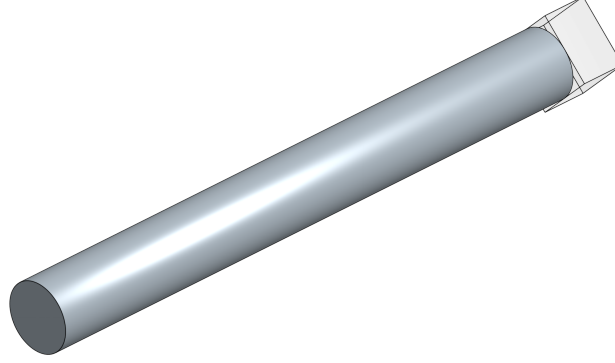


Figure 1: the Design of the Beam,  $\varnothing = 22\text{mm}$  and  $l = 200\text{mm}$

To start, a model was created for each length  $l$ , and was attached to a solid block as a reference frame. The 200mm long beam can be seen in Figure 1 And for each block, the Finite Element simulation was run 9 times, once per energy  $E$  and length  $l$  value.

$l$	$E$	$f$	$\epsilon$	$\frac{1}{l^2}$
100mm	5 J	1536 Hz	1.434 mm	$10^{-4} \text{ mm}^{-2}$
100mm	7.5 J	1536 Hz	1.756mm	$10^{-4} \text{ mm}^{-2}$
100mm	10 J	1536 Hz	2.028mm	$10^{-4} \text{ mm}^{-2}$
150mm	5 J	694.2 Hz	2.601mm	$4.44 \times 10^{-5} \text{ mm}^{-2}$
150mm	7.5 J	694.2 Hz	3.185mm	$4.44 \times 10^{-5} \text{ mm}^{-2}$
150mm	10 J	694.2 Hz	3.678mm	$4.44 \times 10^{-5} \text{ mm}^{-2}$
200mm	5 J	392.9 Hz	3.981mm	$2.5 \times 10^{-5} \text{ mm}^{-2}$
200mm	7.5 J	392.9 Hz	4.876mm	$2.5 \times 10^{-5} \text{ mm}^{-2}$
200mm	10 J	392.9 Hz	5.630mm	$2.5 \times 10^{-5} \text{ mm}^{-2}$

Table 2: the FEA Results

The readings from the simulation was put into Table 1 and as expected, initial energy  $E$  shows no correlation with the frequency  $f$ , and the second part of (1) has been shown true.

For the first part of (1), the modeling of  $\frac{1}{l^2}$  in relation to  $f$  is required, so for each value of  $l$ , and calculating it for each of gives the  $\frac{1}{l^2}$  column of Table 1 and the unit analysis regarding the unit of  $\frac{1}{l^2}$  is given in (9).

Given:

$$\begin{aligned} l &= [\text{mm}] \\ l^2 &= [\text{mm}^2] \end{aligned} \tag{9}$$

Thus:

$$\frac{1}{l^2} = [\text{mm}^{-2}]$$

According to (1),  $\frac{1}{l^2}$  and  $f$  should be proportional, in other words, when graphed, the best line of fit should be a straight line crossing the origin, or in mathematical terms,  $f \approx k\frac{1}{l^2}$  where  $k$  is arbitrary. Doing the regression analysis, using “LibreOffice Calc”, we get  $f = 15226342\frac{1}{l^2} + 13.9$ , or  $f \propto \frac{1}{l^2} + 9.1 \times 10^{-7}$  and the coefficient of determination is  $R^2 = 0.99998$ , showing strong correlation as seen in Figure 2

Where  $l$  is the length of the beam.

While the result is off by  $9.1 \times 10^{-7}$ , this error is small enough in magnitude to be negligible.

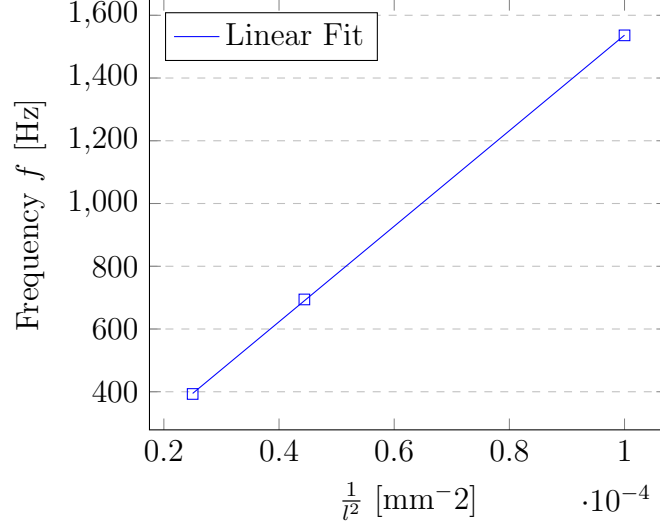


Figure 2: Plot of  $(\frac{1}{l^2}, f)$  and the Linear Fit Line

### 3.3 Experiment

As shown in Section 3.2, the results of the Finite Element Analysis follow the expected relation in Section 3.1. And thus, this experiment aims to replicate the simulation setup used previously, and show that (a) The natural frequency values match those from Table 1 and (b) the natural frequency follows the model as shown in equation (1).

The the initial energy loaded into the material will be controlled by the height of the hammer  $h$  as given by the gravitational potential energy, as shown in (10).

$$E = mgh \quad (10)$$

Where  $E$  is the energy of the hammer,  $m$  is the mass of the hammer and  $h$  is the height.

To calculate the energy of the hammer,  $m = 2 \text{ kg}$  and  $g = 9.81 \text{ms}^{-2}$  is substituted in (10) to get (11), additionally, the units of  $h$  has been converted to meters.

$$E = \frac{h}{1000} 9.81 \times 2 \quad (11)$$

$$E = 0.01962h \text{ J}$$

The table Of variables as seen in Table 1 is similar to Table 1, found in Section 3.2 but a few changes were made to facilitate the experiment, notably, the deformation of the material  $\epsilon$  is no longer measured, because of the difficulty that arises from trying to measure it while leaving frequency  $f$  unaffected. And finally, hammer height has been added as a variable, this is the method for controlling the initial energy load  $E$  for the analysis.

The same values for  $\varnothing$ ,  $l$  and  $E$  will be used as (7) in Section 3.2, the values for  $h$  will be calculated according to (11), shown in (12).

$$\begin{aligned}
5 \text{ J} &= 0.01962h_1 \\
h_1 &= 254.8 \text{ mm} \\
h_2 &= 382.2 \text{ mm} \\
h_3 &= 509,6 \text{ mm}
\end{aligned}
\tag{12}$$

Where  $h$  is the height of the hammer.

Variable	Length $l$	Energy $E$	Hammer Height $h$	Frequency $f$
Type	Independent Discrete	Independent Discrete	Independent Discrete	Dependent Continuous
Unit	mm	J	mm	Hz, $\text{s}^{-1}$
Control	Calipers	Calculated from $h$	Calipers	Fourier Transform

Table 3: Table Of Variables for the Experiment

The setup of the experiment is shown in Figure 3, the height of the hammer is specifically chosen so the corner of the hammer hits the corner of the metal bar, to ensure the bar is excited the same way every time.

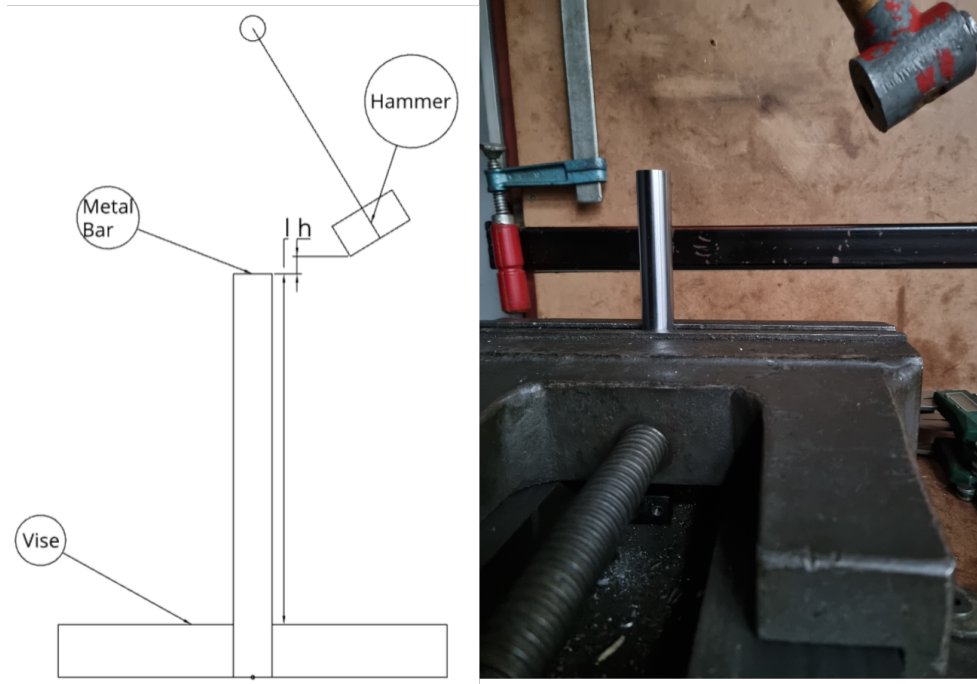


Figure 3: the Experiment Setup

To analyze the data, the Fast Fourier Transform was used, as explained in Section 2.3, to convert the time-pressure graphs, also known as waveforms from the sound recording, such as the one seen in Figure 4 into the frequency domain, as shown in Figure 5

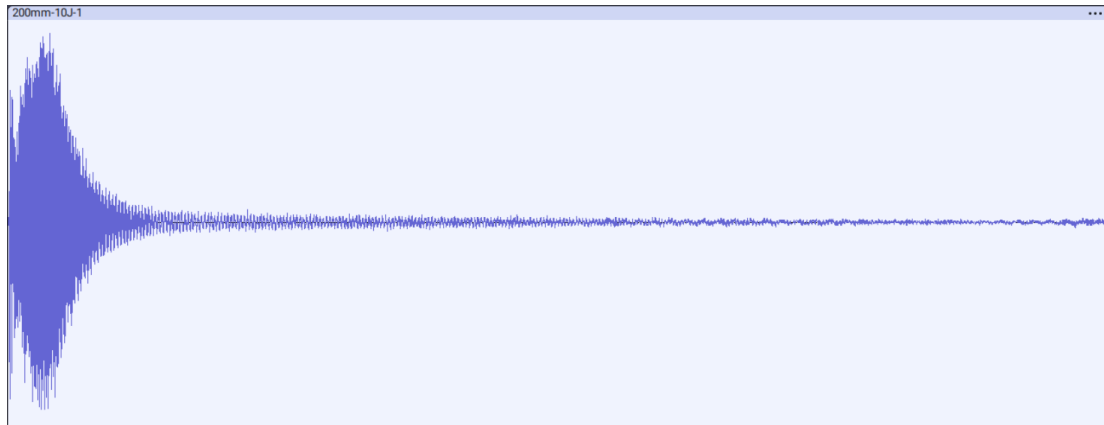


Figure 4: the Recording From  $E = 10$  J and  $l = 200$  mm

For consistency, a 1 second section following the immediate peak (caused by the initial collision with the hammer) was taken from each recording, divided into 32768 time-pressure

samples and the data was put through the Fast Fourier Transform algorithm, more specifically, the “Spectrum” algorithm in the Frequency Analysis tool in the open source audio processing program “Audacity”.

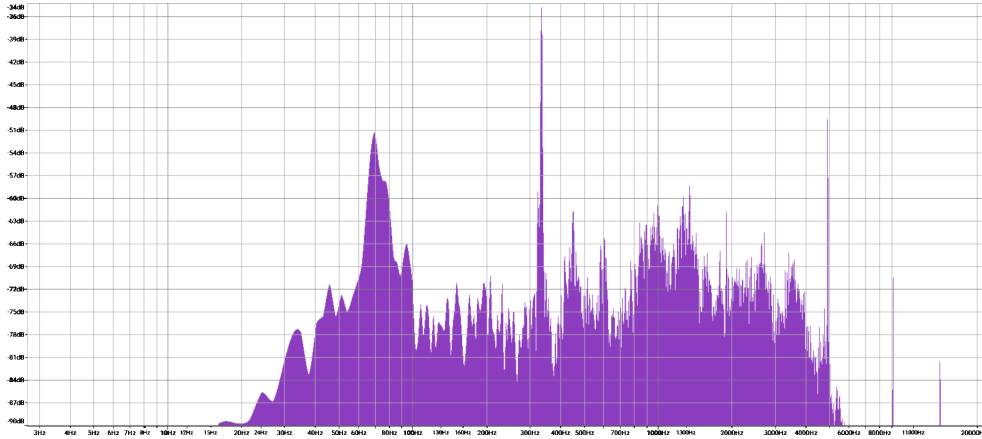


Figure 5: Frequency-Amplitude Graph Attained From the Analysis(Log Scale) There is a clear peak at 334 Hz.

Each set of length and energy was ran 3 times to determine the magnitude of random error in the experiment. After putting every single recording through the Fast Fourier Transform algorithm and picking the peak frequency for each one, the results are seen in Table 4.

$l$	$\frac{1}{l^2}$	$E$	$f_1$	$f_2$	$f_3$	$f_{mean}$
100mm	$10^{-4} \text{ mm}^{-2}$	5 J	956 Hz	913 Hz	907 Hz	$925 \pm 2.98 \text{ Hz}$
100mm	$10^{-4} \text{ mm}^{-2}$	7.5 J	913 Hz	933 Hz	936 Hz	$927 \pm 2.04 \text{ Hz}$
100mm	$10^{-4} \text{ mm}^{-2}$	10 J	914 Hz	927 Hz	895 Hz	$912 \pm 2.32 \text{ Hz}$
150mm	$10^{-4} \text{ mm}^{-2}$	5 J	563 Hz	539 Hz	563 Hz	$555 \pm 2.15 \text{ Hz}$
150mm	$10^{-4} \text{ mm}^{-2}$	7.5 J	536 Hz	539 Hz	564 Hz	$546 \pm 2.26 \text{ Hz}$
150mm	$10^{-4} \text{ mm}^{-2}$	10 J	540 Hz	534 Hz	540 Hz	$538 \pm 1.07 \text{ Hz}$
200mm	$10^{-4} \text{ mm}^{-2}$	5 J	335 Hz	335 Hz	324 Hz	$331 \pm 1.45 \text{ Hz}$
200mm	$10^{-4} \text{ mm}^{-2}$	7.5 J	335 Hz	334 Hz	334 Hz	$334 \pm 0.44 \text{ Hz}$
200mm	$10^{-4} \text{ mm}^{-2}$	10 J	334 Hz	334 Hz	332 Hz	$333 \pm 0.62 \text{ Hz}$

Table 4: the Values from the Finite Element Analysis.

Looking at Table 4, It is clear that  $E$  and  $f$  have no relation, as suggested in (1) and simulated in Section 3.2, with this, every subsequent section will only take recordings where  $E = 10 \text{ J}$  into account.

In a similar manner to Figure 2, the data in Figure 4 has been graphed and a linear fit line has been calculated, and shown in Figure 6. From the analysis, the values  $R^2 = 0.97809$  showing strong correlation and  $f = 7605636\frac{1}{l^2} + 170$  were acquired, or transformed to  $f \propto \frac{1}{l^2} + 2.2 \times 10^{-5}$

While the result is once again, off by  $2.2 \times 10^{-5}$ , it is small enough to be negligible.



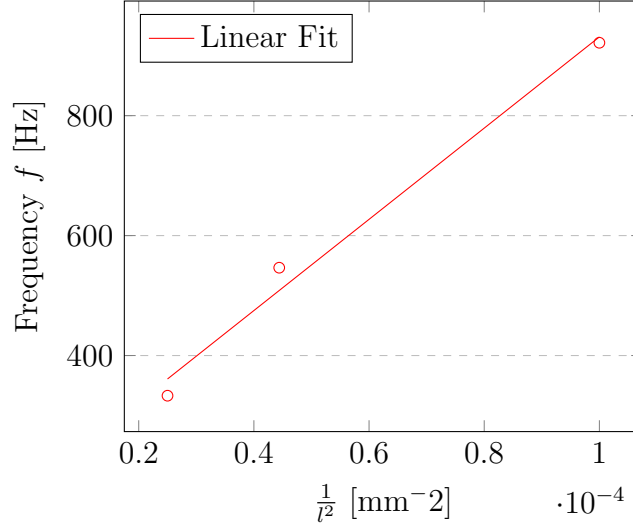


Figure 6: Table of  $(\frac{1}{l^2}, f)$  and linear regression

## 4 Results And Analysis

### 4.1 Uncertainty Analysis

In both Section 3.2 and Section 3.3, where the same experiment was conducted on a simulation and a physical experiment, there exists several sources of uncertainty that can influence the results. For the Finite Element Analysis, the primary source is the mesh resolution. Since Onshape automatically generates the mesh, the level of refinement and its impact on frequency values was not systematically investigated. According to Onshape, the “Variance of frequency analysis is within 0.1 Hz for simple structures.” (Brown and Onshape 2022).

The material properties used in the analysis are nominal values for the hardened carbon steel material and the actual material properties of the physical beams used might have some small differences, contributing to systematic error. The boundary conditions in simulation are idealized as perfectly fixed, while in reality, the vise has introduced some compliance and damping, as it can be seen from Figure 4, the magnitude of the noise

quickly decreases, also contributing to the systematic error not found in the idealized simulation.

In the experiment, length measurements using calipers have a precision limit, while relatively tiny, it introduces a small uncertainty in  $\frac{1}{l^2}$  values. Controlling the initial energy was also dependent on the mass and the height measurements of the hammer, but consistency in hammer drop and energy transfer is imperfect and it also introduced some random error. The rigidity of the vise and the damping at the fixture point also has also introduced additional random uncertainties. Finally, identifying the resonant frequency from the Fourier Transform plots involves a degree of subjectivity and precision limitations in peak frequency determination. These uncertainties, from both the Finite Element Analysis and experiment, should be considered when interpreting and comparing the results, and were included in the Tables and values where possible.

## 5 Discussion

The findings from both the simulation and experimental methods generally support the hypothesis, that the resonant frequency of a the beam is inversely proportional to the square of its length and is independent of the initial energy. Regression analysis of both the simulation and experimental data gave high  $R^2$  values, 0.99998 and 0.97809 respectively, for the linear relationship between frequency and  $\frac{1}{l^2}$ , indicating a strong correlation. However, the experimental frequencies are consistently lower than those predicted by the simulation for each set of beams. This discrepancy could be attributed to systematic error, coming from factors including material property variations, the imperfect vise fixture in the experiment, and also the imperfect Fourier Transform.

The nonzero Y axis intercept in both the simulation and experiment (13.9 and 170 respec-

tively), an order of magnitude larger on the experiment compared to the simulation, this suggests a systematic error on both. This indicates an underestimation of frequency at longer lengths, or might reflect limitations of the simple linear model at lower frequencies. The near-negligible effect of initial energy on resonant frequency was confirmed by both the Finite Element Analysis and experiment, matching the theory. The systematic error could also be caused by the width of the beam being non-negligible width.

To improve this investigation, the experimental setup could be improved for more consistent energy input and fixture rigidity. other studies could explore beams of different materials or cross-sections to test the broader applicability of the observed relationships, and additionally could individually test material properties for it to match the simulation more closely.

## 6 Conclusion

This investigation aimed to determine the amount to which the length of a circular cantilever beam would affect its resonant frequency and to show the capability of the theoretical model. Both Finite Element Analysis and experimental results demonstrate a clear relationship between the resonant frequency and the length of the beam, supporting the theoretical prediction and the first part of the research hypothesis. The initial impact energy was shown to have a no predictable effect on the frequency, confirming the second part of the hypothesis as well.

The theoretical model, implemented through Finite Element Analysis, provides an accurate prediction of the resonant frequency behavior with varying length, although it seems to overestimate the frequency values compared to experimental results. In answer to the research question, changing the length significantly affects the resonant frequency in a

predictable manner, and the hypothesis this relationship, with the possibility for further improvement in both simulation parameters and experimental methodology. Future work should aim to address the identified limitations to further confirm and refine the understanding of the cantilever beam dynamics.

## References

- Bao, M. (Apr. 2005). *Analysis and Design Principles of MEMS Devices*. Elsevier Science, p. 328. ISBN: 9780080455624. URL: <https://books.google.com.tr/books?id=No7NNfc1pfYC>.
- Brown, Greg and Onshape (Nov. 2022). *Onshape Simulation is Fundamentally Improving How Product Designers Use CAD and FEA*. Tech. rep.
- Gross, D. et al. (2014). *Engineering Mechanics 3: Dynamics*. Engineering Mechanics. Springer Berlin Heidelberg. ISBN: 9783642537127. URL: <https://books.google.com.tr/books?id=P1LFBAAAQBAJ>.
- Hool, George A. and Nathan C. Johnson (1929). *Handbook of Building Construction*. First. Vol. Vol. 1. McGraw-Hill Book Company, Incorporated, p. 1920.
- Rao, K.R., D.N. Kim, and J.J. Hwang (2011). *Fast Fourier Transform - Algorithms and Applications*. Signals and Communication Technology. Springer Netherlands. ISBN: 9781402066290. URL: <https://books.google.com.tr/books?id=48rQQ8v2rKEC>.
- Zienkiewicz, O.C. and R.L. Taylor (2000). *The Finite Element Method: Solid mechanics*. Vol. 2. Butterworth-Heinemann, p. 459. ISBN: 9780750650557. URL: <https://books.google.com.tr/books?id=MhgBfMWfVHUC>.